

Measurement of Residual Stresses with Optical Techniques

J. Ribeiro*, J. Monteiro[‡], M. Vaz[†], H. Lopes* and P. Piloto*

*Instituto Politécnico de Bragança, Bragança, Portugal

[†]Faculdade de Engenharia da Universidade do Porto, Porto, Portugal

[‡]Instituto de Engenharia Mecânica e Gestão Industrial, Leça do Balio, Portugal

ABSTRACT: The goal of this work was the development of other experimental techniques to measure residual stresses, as an alternative to the hole-drilling method with strain gauges. The proposed experimental techniques are based on the use of Moiré interferometry and in-plane electronic speckle pattern interferometry (ESPI). Both are field techniques allowing the assessment of in-plane displacements without contact and high resolution. Grating replication techniques were developed to record high-quality diffraction gratings onto the specimen's surfaces. An optical set-up of laser interferometry was developed to generate the master grating (virtual). An in-plane ESPI set-up was also designed and implemented to measure displacements in one direction. The stress relaxation was promoted by the blind hole-drilling and the obtained fringe patterns (Moiré and speckle) were video-recorded. Image processing techniques were applied to assess the in-plane strain field. A finite-element code (ANSYS®) was used to simulate the stress relaxation process, whose values were compared with the experimental data, and to calculate the hole-drilling calibration constants.

KEY WORDS: *electronic speckle pattern interferometry, finite-element method, hole drilling, Moiré interferometry, residual stresses*

Introduction

Residual stresses are the ones that remain on components and structures after the load has been removed. These may result from fabrication processes such as welding and machining, or due to overload localised yielding. Usually these stresses are undesirable because they added to service stresses reducing the structures maximum load. However, when variable loads are expected compression surface residual stresses are sometimes applied to improve fatigue resistance. This way the residual stress assessment assumes a very important role in mechanical design.

The frequently used technique for residual stress measurement is the hole-drilling method with strain gauges. In this case, three discrete measurements were used to obtain the stress released during the hole drilling. Special rosettes and drilling devices are used for this propose according to the ASTM standard [1]. This standard describes the methodology and the limits of the measurements according to the expected in-depth stress distribution. Other techniques are also available based on the measurements of deformations at the crystallographic and macroscopic levels.

Nowadays, image techniques have experienced a great improvement in what concerns experimental mechanics applications. Displacement fields can be assessed by non-contact techniques with high resolution by using ordinary white light or laser illumination. Image correlation [2], geometric and interferometric Moiré [3], speckle or holographic interferometry [4] are available with resolutions up to the laser wave length.

In this work, a new process to measure residual stresses with optical techniques (in-plane ESPI and Moiré interferometry) was developed and combined with the hole-drilling method. Measurements were carried out on a ring and plug specimen, constructed to produce well-known residual stress fields. The calibration coefficients were obtained by numerical simulation with a finite-element method (FEM) code generated in the ANSYS® programme.

An image processing software package was developed at Laboratory of Optics and Experimental Mechanics (LOME) to calculate the displacement field from the interferometric patterns. Moiré interferometry technique was used in the second test after replication of a grating with 1200 L mm^{-1} on the

specimen surface. A set-up to measure the in-plane displacement field in two directions was prepared and used.

Residual Stress Measurement Set-ups

In this work, two optical set-ups were prepared, one for Moiré interferometry [5] and the other for double-illumination ESPI [6]. Both were used to measure the in-plane displacements generated by residual stress release. Image processing algorithms, involving filtering, phase calculation and unwrapping, and spatial differentiation were used in data post-processing to transform surface displacement into residual stress fields. In Figure 1 a schematic presentation of the two optical set-ups used can be seen.

The stresses were released according to the conventional procedure used with strain gauges. Drilling a

hole on the surface of a specimen with residual stresses produces a stress relaxation around it. The corresponding deformation was assessed in this work with an optical technique. The stress analysis algorithms are based on the work of Nelson [8, 9] and Wu [10], adapted to work with ESPI and Moiré interferometry data.

The light source used in both set-ups was a 2-W laser from Coherent (Verdi). For image acquisition, a CCD Sony XC-8500CE camera with 782 × 582 pixel of resolution was selected. A computer-controlled PI piezoelectric actuator was used to perform the phase modulation needed to calculate the phase maps using the algorithm described by Creath [11]. Finally, a dedicated support was constructed with a 10-μm resolution Microcontrol linear stage to allow depth control drilling. With this support, the air turbine used as drill could be removed and replaced with minor chances in its alignment.

In the ESPI measurement, an initial specklegram is acquired and saved. Then, the drill is placed in front of the test specimen and a small hole is drilled to a given depth. Next, the drill is removed and another specklegram is acquired. The interferogram resulting from the correlation of the two recordings leads to the surface displacements caused by the stress relaxation. In this case, the surface information is codified in the speckle patterns.

For the Moiré interferometry, a high-frequency grating is previously bonded on the surface of the specimen. The grating used was of 1200 lines per millimetre, obtained by aluminium vaporisation on top of an epoxy replication of a master grating from photomechanics. The followed replication process is described by Wu [12]. The set-up proposed by Post [13] was used in the virtual grating generation by laser interferometry. The first recording was obtained by superposition of the virtual grating over the object replication grating. Then, a hole is drilled at the desired place, and the Moiré fringes due to stress relaxation are obtained and recorded. A tiltable parallel plate glass was used to promote phase modulation with a four image phase calculation algorithm [11].

In both cases, the residual stress field was computed establishing an appropriate stress–displacement relationship by a FEM code. According to Nelson [8], the displacements due to residual stress relaxation are related between themselves through the following equations,

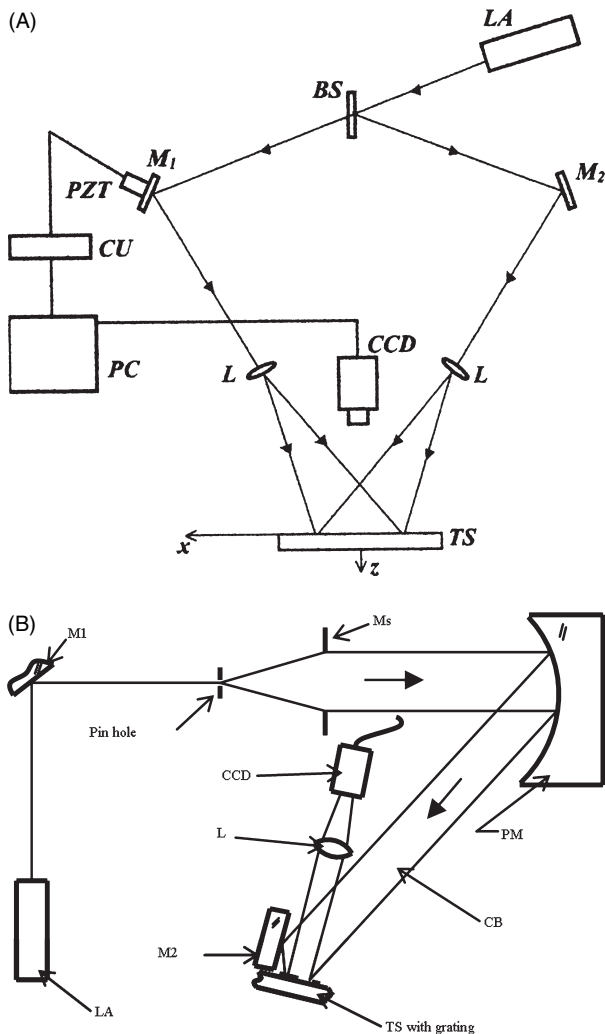


Figure 1: Schematic presentation of the optical set-ups used: (A) in plane ESPI [6]; (B) Moiré interferometry [7]. LA is the laser source, BS is a beam splitter, M1 and M2 are plane mirrors, PZT is a piezoelectric phase modulation device, L is a lens, TS is the test specimen, Ms is a mask, CB is the collimated beam and PM is a parabolic mirror

$$u_r^k = \begin{bmatrix} A + B \cos 2\theta_k \\ A - B \cos 2\theta_k \\ 2B \sin 2\theta_k \end{bmatrix}^{-1} \begin{bmatrix} \sigma_{xx} \\ \sigma_{yy} \\ \tau_{xy} \end{bmatrix} \quad (1a)$$

$$u_{\theta}^k = \begin{bmatrix} C \sin 2\theta_k \\ C \sin 2\theta_k \\ 2C \cos 2\theta_k \end{bmatrix}^{-1} \begin{bmatrix} \sigma_{xx} \\ \sigma_{yy} \\ \tau_{xy} \end{bmatrix} \quad (1b)$$

where u_r^k and u_{θ}^k are, respectively, the radial and tangential displacements; k the number of measured points; A , B and C the calculated coefficients depending on the material elastic constants, the hole dimensions (diameter and depth) and the radial position around the blind hole; θ_k is the cylindrical coordinate of the measurement point and σ_{xx} , σ_{yy} and τ_{xy} are stress components in Cartesian coordinates. When optical techniques are used, the number of measured points can be selected from the information contained in the recorded image, this way the residual stresses can be obtained from the hole edge until the image border.

The A , B and C coefficients can be obtained by different ways: experimental, analytical and numerical determination. The experimental methods are the most accurate ones; however, they are time consuming when compared with analytical and numerical methods, more expensive because they only can be used for a certain hole geometry and strain gauge rosette. The analytical methods are based in many simplifications that, in certain cases, do not represent the reality and can only be used for the case of uniform residual stresses. The numerical methods are more generic; they can simulate any field of residual stresses; it is possible to determine coefficients for different hole-drilling techniques: incremental strain method, power series method, integral method, average stress method, ASTM E837 method. In this work, the calibration coefficients were numerically calculated.

Numerical Determination of Calibration Coefficients

The main goal in this simulation was to establish a model that could be used in the determination of the calibration coefficients for different hole-drilling techniques with good accuracy. Thus, a three-dimensional finite-element model was used for the numerical determination of the calibration coefficients following the procedure presented by Lu [14] and Schajer [15], using brick, homogeneous and isotropic elements in the ANSYS® FEM code. A three-dimensional finite-element mesh, with 5525 parametric brick elements (SOLID185) was used, as represented in Figure 2 [7].

To test the described experimental methodology, a calibration specimen was made in aluminium alloy (1050). This alloy (with 90% of Al) was chosen

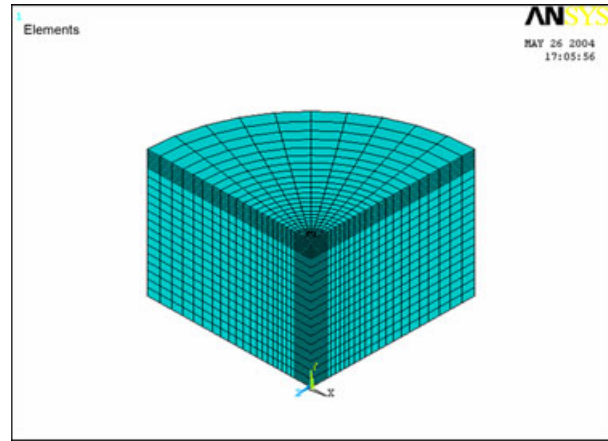


Figure 2: Finite-element method mesh of the three-dimensional model

because it is readily available and well characterised. The material properties and geometric parameters used in this numerical simulation are shown in Table 1.

Two different residual stresses states were considered:

(a) Equi-biaxial: $\sigma_{xx} = \sigma_{yy} = \sigma$, $\tau_{xy} = 0$, the corresponding stresses in cylindrical coordinates are $\sigma_{rr} = \sigma_{\theta\theta} = \sigma$, $\tau_{r\theta} = 0$. This drilling condition is equivalent to a uniform pressure on the surface of hole and it is represented on the left-hand side of Figure 3A.

(b) Pure shear: $\sigma_{xx} = -\sigma_{yy}$, $\tau_{xy} = 0$, the corresponding stresses in cylindrical coordinates are $\sigma_{rr} = \sigma \cos 2\theta$, $\sigma_{\theta\theta} = -\sigma \cos 2\theta$, $\tau_{r\theta} = -\sigma \sin 2\theta$. After the hole drilling, this stress distribution change to an harmonic distribution of radial stresses; being $\sigma_{rr} = -\sigma \cos 2\theta$ and a shear stress $\tau_{r\theta} = \sigma \sin 2\theta$, both acting on the hole edge, as can be seen on the right-hand side of Figure 3B. The signals of the stresses change due to stress release after the hole drilling.

The calibration coefficients were computed with the expressions presented by Wu [10], which, for the case in the analysis lead to:

$$A\left(E, V, r_0, r, \frac{h}{d_0}\right) = \frac{u_r(r, \theta)}{2\sigma} \quad (2a)$$

$$A\left(E, V, r_0, r, \frac{h}{d_0}\right) = \frac{u_r(r, \theta)}{2\sigma \cos 2\theta} \quad (2b)$$

Table 1: Material, geometric and load conditions

σ (MPa)	E (MPa)	ν	r_0 (mm)	h (mm)
100	7.0×10^4	0.3	1.0	0.5

σ is the specified residual stress, E the elastic modulus, ν the Poisson ratio of material, r_0 the hole radius and h the depth.

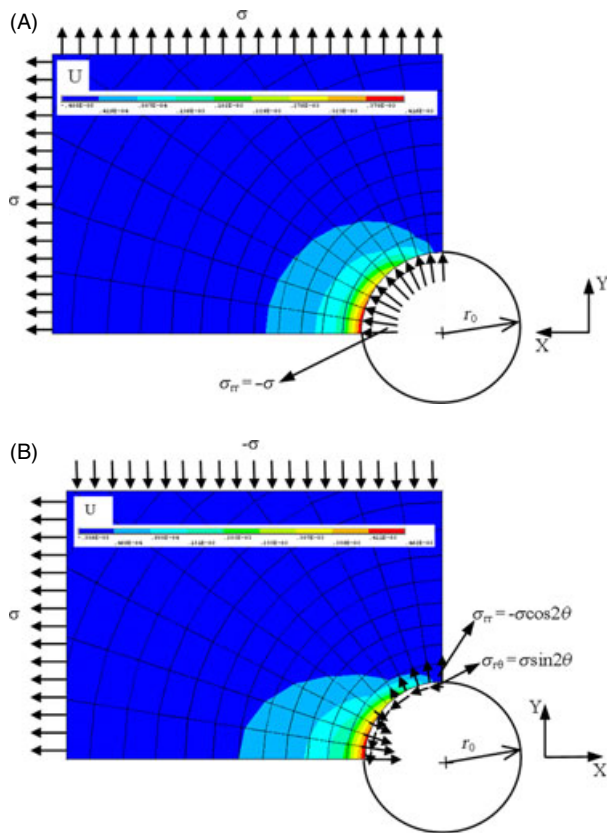


Figure 3: Three-dimensional FEM model for the calibration coefficients determination: (A) equi-biaxial stresses: $\sigma_{xx} = \sigma_{yy} = \sigma, \tau_{xy} = 0$; (B) pure shear stresses: $\sigma_{xx} = -\sigma_{yy}, \tau_{xy} = 0$

$$A\left(E, V, r_0, r, \frac{h}{d_0}\right) = \frac{u_\theta(r, \theta)}{2\sigma \sin 2\theta}. \tag{2c}$$

The calibration coefficients are dimensionless and were computed for a hole with 2 mm in diameter and 0.5 mm depth, at a radial distance of $1.2r_0$ from the centre of the hole. Table 2 summarises the values of calibration coefficients that were obtained. The process was repeated for different diameters: 1.8, 2, and 2.2 mm.

Ring and Plug Specimen

To obtain well-known residual stress fields, an aluminium shrink-fit ring and plug was chosen. This specimen has a closed form solution for the residual stresses, and relatively simple stress distribution. In the plug the stress is constant, and in the ring depends only on the radial position. On the other

Table 2: Calibration coefficients

A	B	C
4.64×10^{-6}	5.88×10^{-6}	3.82×10^{-6}

hand, this type of specimen provides the full range of biaxial stress states: in the ring near the interface, σ_θ is positive and σ_r is negative, near the outer edge the stress state is nearly uniaxial, (as σ_r tends to zero), in the plug, the stress state is equi-biaxial, $\sigma_\theta = \sigma_r$. On the other hand, the residual stresses in the specimen are uniform in depth; thus, it is possible to use the ASTM standard [1]. Therefore, with only a specimen it is possible to demonstrate the ability of the optical technique on three different residual stress conditions [16], and several measurements could be performed.

The nominal dimensions of the specimen used were 100 and 50 mm for the exterior and interior diameter of the ring respectively. The thickness of both elements was 13 mm and they were assembled with a radial interference of 0.05 mm.

To control the assemblage conditions, two strain gauges were bonded at the same radial distance (30 mm) but oriented in two orthogonal directions (tangential and radial). For assembly, the plug was cooled in liquid nitrogen (-160°C) and the ring heated (40°C) which leaves approximately 0.2 mm of clearance between them. Figure 4 represents the apparatus used in the assembly control.

The stress distribution of the ring and plug can easily be calculated using Lamé equations [17]. First, the pressure p applied due to the interference is obtained by:

$$p = \frac{E\delta (R_0^2 - R_i^2)}{2R_i R_0^2} \tag{3}$$

where p is taken as positive and δ the radial interference between the ring and the plug. In the plug, the stresses are equal to the pressure in the radial and angular directions. For the ring, the stresses in the same directions are calculated as:

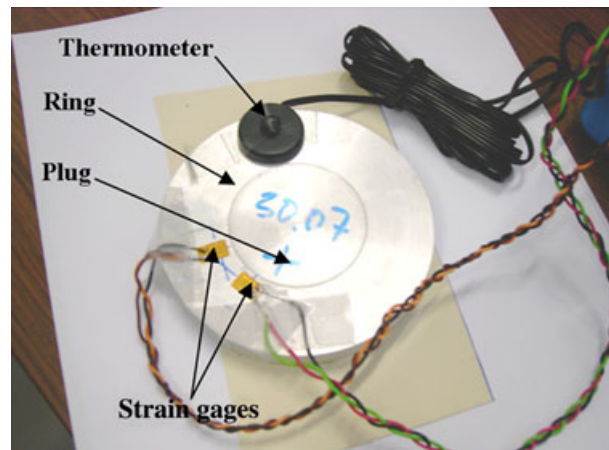


Figure 4: Apparatus used to make the assembly

$$\sigma_r = \frac{pR_i^2}{R_0^2 - R_i^2} \left(1 - \frac{R_0^2}{r^2} \right) \tag{4a}$$

$$\sigma_\theta = \frac{pR_i^2}{R_0^2 - R_i^2} \left(1 + \frac{R_0^2}{r^2} \right). \tag{4b}$$

In the studied case, the pressure due to the radial interference 0.05 mm was 47.3 MPa. With this load, the measurements performed with the strain gauges allow the calculation of the average stresses σ_r and σ_θ , on the strain gauges grid, these values are represented in Table 3. These values are similar to the ones obtained with the closed form solution for the centre of strain gauges grids.

Measurement of Residual Stresses

After the specimen preparation and its stress state control, several measurements of residual stresses were made using optical techniques and the hole-drilling method. The selected points for the residual stress measurements are represented in Figure 5.

To avoid the material influence, the measurements were performed in different angular positions. However, with Moiré interferometry the grating was fixed only on a small part of the specimen and so, only two points were measured. The optical set-up used to measure residual stresses with in-plane ESPI and Moiré interferometry are schematically represented

Table 3: Average stresses σ_r and σ_θ measured by strain gauges

σ_r (MPa)	σ_θ (MPa)
49.9	-30.3

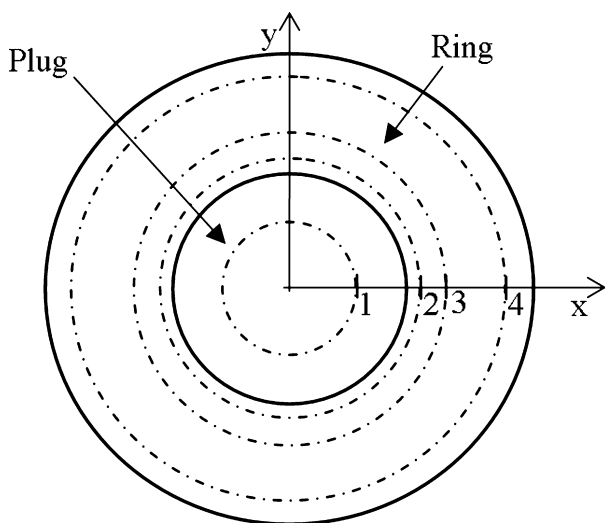


Figure 5: Diametrical location of measurement points

in Figure 1A,B respectively. Figure 6 shows details of both set-ups with the additional system for the hole drilling.

To guarantee hole concentricity and perpendicularity between the drilling apparatus and the measured surface, a conic fixation system was fabricated with a very tight geometrical tolerance. Before the measurements were performed, some tests were carried out to verify hole geometry. After drilling, the holes were measured with an optical microscope in its main dimensions: depth and diameter.

Results

To obtain the displacement field, eight images should be recorded in both techniques, at different phase shifts, half of them before and the remaining after hole drilling. In ESPI, the displacement field is calculated by subtracting the speckle phase maps obtained before and after strain relaxation. One of these measurements, obtained after the hole had been drilled, is presented in Figure 7A,B. The

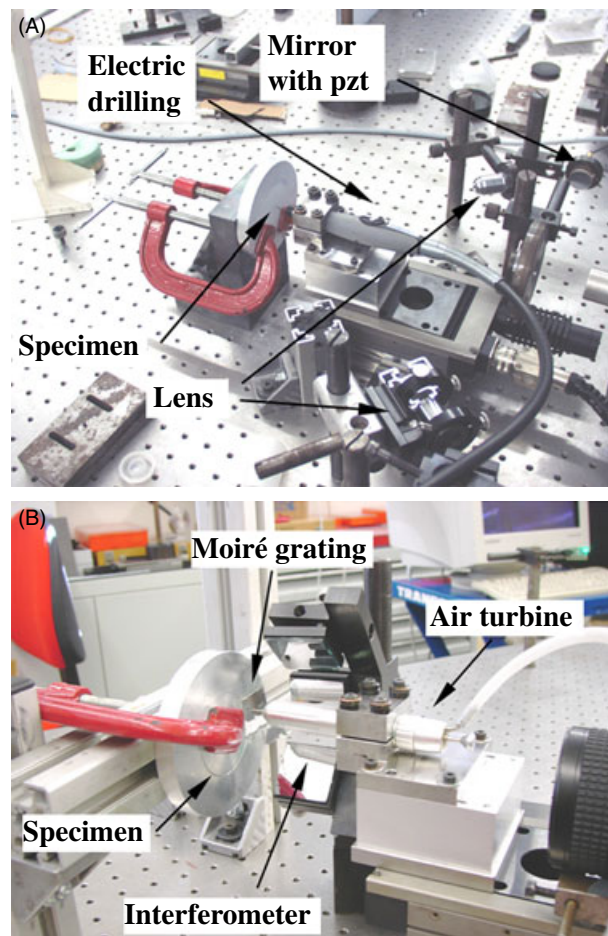


Figure 6: Apparatus to measure residual stresses using the hole-drilling technique associated with: (A) in-plane electronic speckle pattern interferometry; (B) Moiré interferometry

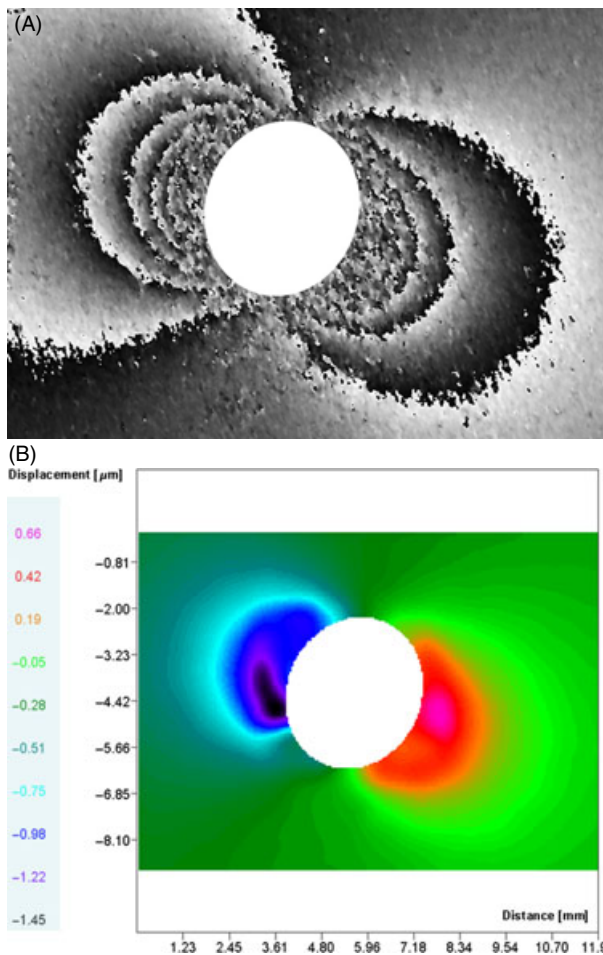


Figure 7: (A) Phase map and (B) unwrapped phase map of displacement field

discontinuities in Figure 7A are due to phase calculation and can be removed by phase unwrapping. Different solutions are available for this proposes according to the data spatial noise. The results presentation could be improved using a pseudo colour presentation where the displacement intensity is codified according to a colour table.

Using the unwrapped phase map corresponding to the displacement field and the calibration coefficients, the residual stresses can be computed using the data obtained for three different points at the same radial distance from the hole centre. The results presented in this work were obtained using three points placed according to Figure 8.

Figure 9 summarises the results obtained for residual stress measurements. In this graphical presentation, the lines represent the stresses calculated by the closed form solutions given by Lamé. The experimental data are represented by dots. In all the cases, the error was less than 15%, most of the measurements were around 5% of error.

For the Moiré interferometry set-up, only the phase modulation device differs from the previous one. In this case, the 90° phase shift between each image was

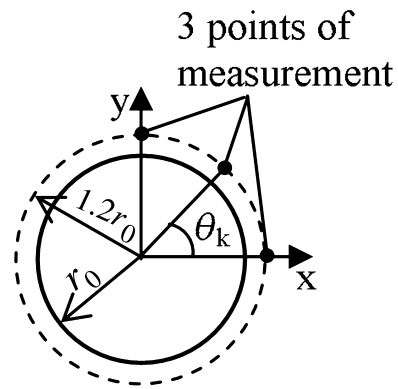


Figure 8: Points of measurement. r_0 is the hole radius and θ_k the angular position of the measurement point. The residual stresses were calculated with equations (1) and the calibration coefficients were computed with equations (2)

performed by the rotation of a glass plate with parallel faces, instead of using a linear displaceable mirror. It should be mentioned that noisy recordings may be obtained if the grid is not properly bonded or has poor quality. Low contrast or poor reflectivity is the most important problem with grid replication, meanwhile a constant glue thickness should be achieved. To obtain the phase maps, filtering and smoothing algorithms should be involved to deal with noisy data. In Figure 10A,B, an example of the phase map around the hole and the computed displacement field after image processing (unwrapping) is presented.

The procedure to compute the residual stresses using the unwrapped phase map of displacement field was the same described for ESPI technique. The results obtained after two measurements in the specimen with Moiré interferometry are presented in Figure 11. In this case, only two measurements were made due to the size of the grid used and the necessary distance between holes to avoid influence between them. In all the measurements an error less than 17% was obtained.

All the holes were drilled in four incremental steps according to the ASTM standard. The final geometry of the holes was verified with a microscope tube with a scaled reticule, they were circulars and the diameters were between 2 and 2.1 mm. Some holes were randomly chosen to cut and verify its sectional geometry, the hole bottom was flat and there was a perpendicularity between the bottom and wall directions of the hole.

Conclusions

In this work, an experimental methodology for residual stress assessment is presented using optical techniques with the hole-drilling method. These methods were tested with a well-known residual

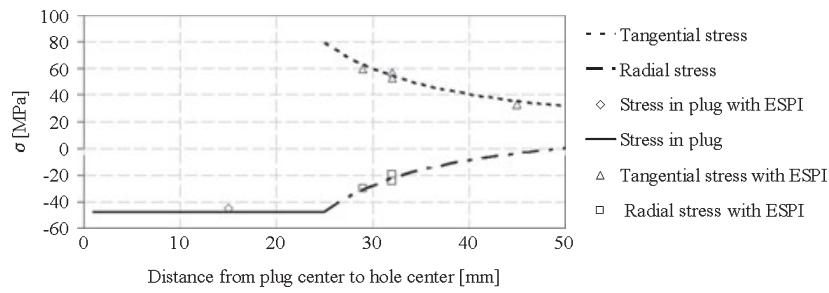


Figure 9: Closed form solution and experimental measurements with ESPI

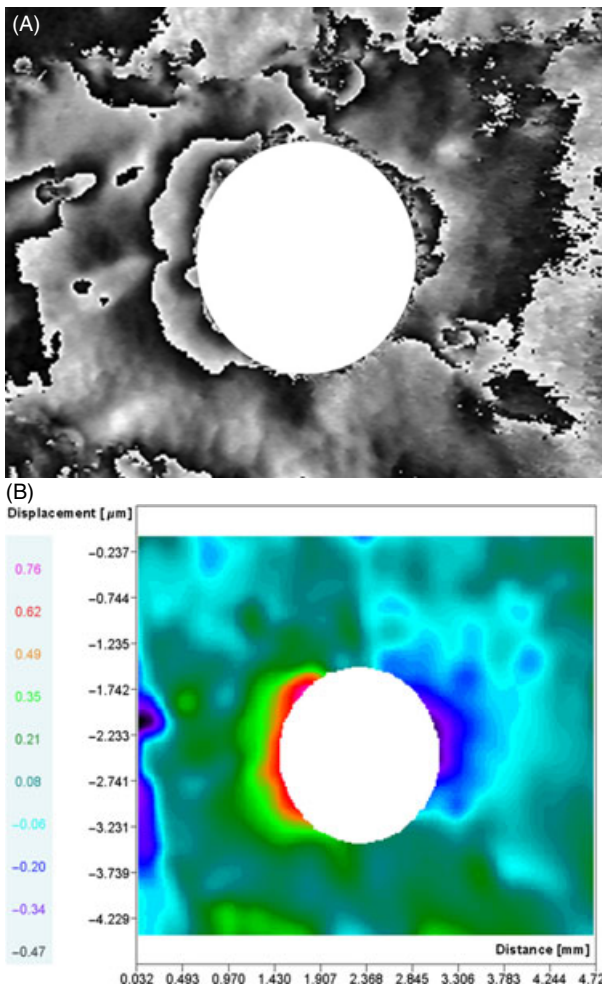


Figure 10: (A) Phase map and (B) unwrapped phase map of displacement field

stress field in a ring and plug specimen. The experimental results obtained with in-plane ESPI and Moiré interferometry are in good agreement with the closed form solution. These optical techniques are a very interesting alternative to the traditional hole-drilling method with strain gauges, and present some advantages, it is a global measurement, has better resolution and allows measurements closer to the hole edge. Image processing algorithms are available to convert the displacement data obtained to values of residual stresses through a series of calibration coefficients obtained by FEM simulation.

REFERENCES

1. Annual book of ASTM standards (2003) *Determining of residual stress by the hole drilling strain gauge method. E837-01e1*. ASTM International, West Conshohocken, PA: 694–703.
2. Nelson, D. V., Makino, A. and Schmidt, T. (2006) Residual stress determination using hole drilling and 3D image correlation. *Exp. Mech.* **46**, 31–38.
3. Min, Y., Hong, M., Xi, Z. and Lu, J. (2006) Determination of residual stress by use of phase shifting moiré interferometry and hole-drilling method. *Opt. Lasers Eng.* **44**, 68–79.
4. Schajer, G. S. and Steinzig, M. (2005) Full-field calculation of hole drilling residual stresses from electronic speckle pattern interferometry data. *Exp. Mech.* **45**, 526–532.
5. Post, D., Han, B. and Ifju, P. (1997) *High Sensitivity Moiré: Experimental Analysis for Mechanics and Materials*. Chapter 4. Springer Verlag, Berlin: 135–226.
6. Jones, R. and Leendertz, J. A. (1974) Elastic constant and strain measurement using a three beam speckle pattern interferometer. *J. Phys. E Sci. Instrum.* **7**, 653–657.

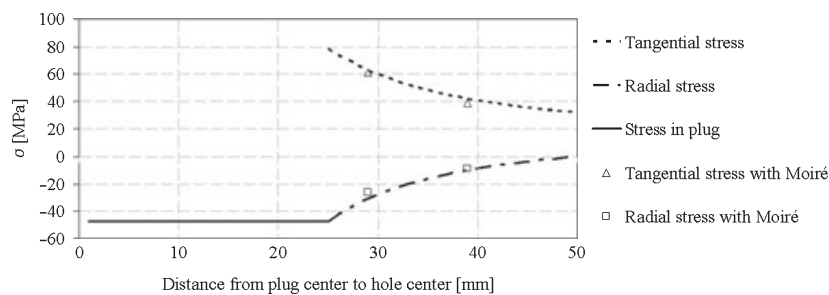


Figure 11: Closed form solution and experimental measurements with Moiré

7. Ribeiro, J., Vaz, M., Piloto, P. and e Monteiro, J. (2005) Técnicas de Medição de Tensões Residuais. *VI Encontro Nacional da Associação Portuguesa de Análise Experimental de Tensões (APAET), nos Proc.* Ponta Delgada.
8. Nelson, D. V. and Makino, A. (1997) The holographic-hole drilling method for residual stress determination. *Opt. Lasers Eng.* **27**, 3–23.
9. Nelson, D. V. and McCrickerd, J. T. (1986) Residual-stress determination through combined use of holographic interferometry and blind hole drilling. *Exp. Mech.* **26**, 371–378.
10. Wu, Z., Lu, J. and Han, B. (1998) Study of residual stress distribution of Moiré interferometry and incremental hole drilling. *J. Appl. Mech.* **65**, 837–850.
11. Creath, K. and Schmit, J. (1996) N-point spatial phase-measurement techniques for non-destructive testing. *Opt. Lasers Eng.* **24**, 365–379.
12. Wu, Z. (1998) Détermination des contraintes résiduelles par interférométrie de Moiré et méthode de perçage du trou incrémental, *Thèse présentée pour l'obtention du grade de Docteur.* Université de Technologie de Troyes, Troyes.
13. Czarnek, R. and Post, D. (1984) Moiré Interferometry with $\pm 45^\circ$ Gratings. *Exp. Mech.* **45**, 68–74.
14. Lu, J., James, M. R. et al. (1996) *Handbook of Measurement of Residual Stresses* (J. Lu, Ed.). The Fairmont Press, Lilburn, GA: 5–34.
15. Schajer, G. S. (1981) Application of finite element calculations to residual stress measurements. *J. Eng. Mater. Technol.* **103**, 157–163.
16. Steinzig, M., Hayman, G. and Prime, M. (2001) Verification of a Technique for Holographic Residual Stress Measurement. *ASME Pressure Vessels and Piping Conference, Published in Residual Stress Measurement and General Non-Destructive Evaluation*, Vol. 429, Atlanta.
17. Lamé, M. G. (1852) *Leçons sur la Théorie Mathématique de l'Élasticité des Corps Solids.* Bachelier, Paris.